INFLUENCE OF PRE-CURING STAGE IN ADDITIVE MANUFACTURING OF ADVANCED THERMOSETTING COMPOSITES

Francesco, Taddei[a], Michel, Barbezat[a], Enrico, Troiani[b], Giacomo, Struzziero[a]

a: Laboratory for Mechanical Systems Engineering, Swiss Federal Laboratories for Materials Science and Technology (Empa), Überlandstrasse 129, 8600 Dübendorf, Switzerland (first author's email: francesco.taddei@empa.ch)
b: Department of Industrial Engineering DIN, University of Bologna, Via Fontanelle 40, 47121 Forlì, Italy

Abstract: *The arising of cure-related defects during manufacturing of thermosetting composites and their hardly predictable effect on mechanical-performance is often cause for part rejection, which is detrimental for both cost and sustainability. Additive Manufacturing (AM) of continuous fibre-reinforced thermosets is envisaged to bring significant benefits in terms of reducing temperature overshoot, and consequently residual stresses. The work investigates the influence of the introduction of a pre-curing phase upon the exothermic overshoot and the defects induced during deposition of pre-cured tows (i.e. microbuckling). A Finite Element Analysis (FEA) addressing the cure simulation has been developed, and pre-cured specimens have been tested. The findings point out that a pre-cure level between 20% and 30% reduces the temperature overshoot within the laminate by 90%, generating in-plane waviness with a severity that should not compromise its performance.*

Keywords: Additive Manufacturing; residual stresses; exothermic overshoot; pre-curing; in-plane waviness

1. Introduction

Composite materials have considerably expanded their applications due to their excellent mechanical performance together with lightweight. Nevertheless, the high non-linearity of the cure stage often introduces unexpected defects (i.e. thermal gradients, residual stresses, matrix cracking) which undermine part quality and lead to part rejection. Due to the low thermal conductivity through-thickness, the scenario worsens for thicker parts [1-4].

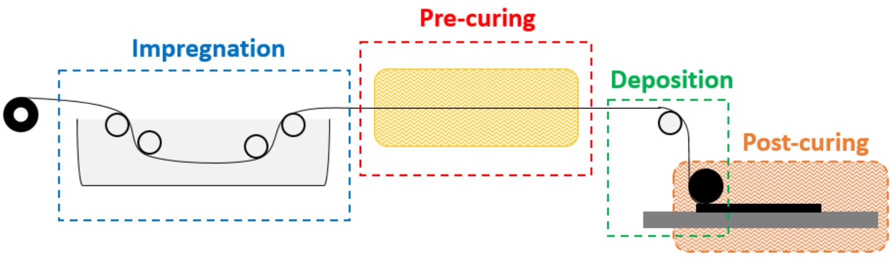

Figure 1. AM process scheme

Additive curing of Carbon/Epoxy composites can strongly reduce the exothermic overshoot during cure and the related residual stresses [5,6]. The addition of a pre-curing stage between the impregnation and deposition units (Fig. 1) shows the potential to further exploit these benefits, allowing for the manufacturing of high-quality thick components and for the design of more aggressive cure cycles with the consequent reduction in process time. However, the deposition of pre-cured tows might induce other stresses inside the material that could result in phenomena like microbuckling [7,8]. This work investigates the twofold influence of pre-curing upon exothermic overshoot and deposition induced defects.

2. Materials and methodology

2.1 Resin system characterization

The resin under characterisation is a system composed of hot-melt epoxy resin XB3515, hardener paste Aradur® 1571 and Accelerator 1573 [9]. Characterization of the cure kinetics and resin specific heat was performed via Differential Scanning Calorimetry (DSC) in isothermal (*90°C*, *100°C*, *110°C*, *120°C*, *140°C*), dynamic (*1°C/min*, *2°C/min*, *10°C/min*, *50°C/min*) and temperature-modulated scans (*3°C/min* with a modulation amplitude of *1°C* every *60 s*) [10,11]. The gel point was estimated using oscillatory mode in a rheometer during isothermal tests with frequencies of *0.5 Hz* and *1 Hz* and temperatures of *100°C*, *110°C*, *120°C* [11]. An autocatalytic model with a diffusion term in Eq. (1) was used to fit experimental data. The glass transition was modelled using the DiBenedetto curve of Eq. (2). Finally, Eq. (3) expresses the specific heat capacity as a function of temperature and degree of cure.

$$\frac{d\alpha}{dt} = \frac{A\cdot\exp(-\frac{E}{R\cdot T})}{1+\exp[C(\alpha-(\alpha_C+\alpha_T\cdot T))]}\alpha^m(1-\alpha)^n \quad (1)$$

$$T_g = T_{g_0} + \frac{(Tg_\infty - Tg_0)\cdot\lambda\cdot\alpha}{1-(1-\lambda)\cdot\alpha} \quad (2)$$

$$C_p = C_r + C_{r_T}\cdot T + \frac{Cg-Cr-Cr_T\cdot T}{1+\exp(C(T-Tg-\sigma-\sigma_T\cdot T))} \quad (3)$$

Where $d\alpha/dt$ is the reaction rate, α the degree of cure, T the temperature, n the 1st reaction order, m the 2nd reaction order, A the pre-exponential Arrhenius factor, E the activation energy, C the coefficient controlling the breadth of the transition, α_C the coefficient governing the chemical-controlled part of the reaction, α_T the coefficient governing the diffusion-controlled part of the reaction, Tg is the glass transition temperature, Tg_0 the glass transition temperature for the uncured resin, Tg_∞ the glass transition temperature for the fully cured material, λ a fitting parameter controlling the convexity of the non-linear regression, C_p is the specific heat, C_r and C_g are respectively the intercepts in the rubbery and glassy state, Cr_T controls the dependence on temperature in the rubbery state, σ, C and σ_T are the parameters governing respectively the position, breadth and temperature dependence of the specific heat transition from rubbery to glassy state.

2.2 Cure simulation

A 1D Heat Transfer (HT) model is built in *Abaqus/CAE* with user-subroutines [1,3,12], governed by the energy balance in Eq. (4).

$$\rho_c C_p \frac{\partial T}{\partial t} = \left(1-v_f\right)\rho_r H_{tot}\frac{d\alpha}{dt} + \nabla\cdot(\overline{K}\,\nabla T) \quad (4)$$

Where H_{tot} is the total heat of reaction and K is the thermal conductivity matrix. The thermal conductivity and thermal properties of the composite have been computed using the laws and the rule of mixtures reported in [3]. The geometry is modelled as a squared-base solid with dimensions *10x10x14.5 mm*, representing the central region of the laminate, and partitioned along the vertical direction in *80* eight-node linear brick elements. For the validation of the model, the temperature profiles recorded on top and at the bottom of the laminate (see Section 2.3) are used as boundary conditions, while the subroutines FILM and DISP are used in all the other simulations. The initial conditions, in particular degree of cure and temperature, are defined using SDVINI. The convection coefficient for the air in the oven is estimated as $h_{conv} = 43$ by tuning it so that the model matches as best as possible the measurement on the top of the laminate. On the sides, insulation is set as a boundary condition (Fig. 2). Sub-material thermal properties and their evolution are implemented in the subroutine UMATHT.

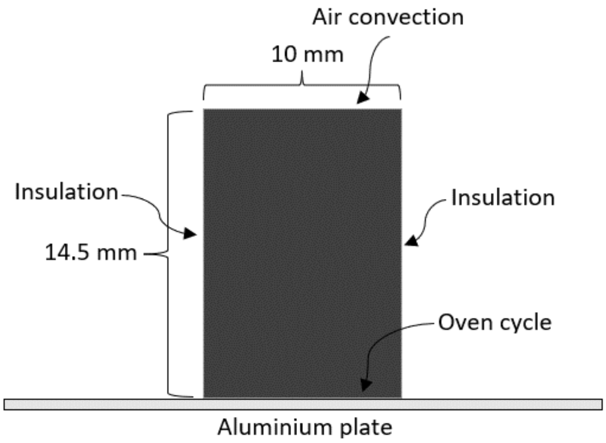

Figure 2. Schematic of geometry and boundary conditions

Once the cure model is built and validated, it can be used to simulate the thermal behaviour of an additively manufactured thermosetting laminate for a certain length (*100 mm*), number of layers (*80* layers of *0.181 mm* each), level of pre-cure (*0-50%*) and printing speed (*600 mm/min*). The model assumes that the HT analysis starts when all the layers have been deposited. However, the initial degree of cure of each layer is estimated through the cure kinetics with a temperature of *120°C,* for duration according to the printing speed selected and thickness position, and fed to the solver as initial condition. Then, the cure is completed by implementing the Manufacturer Recommended Cure Cycle (MRCC).

2.3 Laminates manufacturing

Two UD laminates were manufactured from *80* layers of prepreg strips (*50x100 mm*) for validation of the HT model. The temperature was recorded during every process phase by inserting thermocouples at the bottom, in the middle and on top. One laminate was subjected to the MRCC and its final thickness was *14.5 mm* in the central region where thermocouples were placed. The second laminate was cured with a two-stage procedure: it consisted of pre-curing two sub-laminates made of *40* layers without vacuum bagging up to *26%* and *42%* degree of cure; afterwards, the less cured part was put on top of the other one, and their cure was progressed under vacuum conditions using the MRCC.

2.4 Deposition analysis

Metallic fixtures for a bending test were designed as shown in Fig. 3 to mimic the deposition process. Their geometry mimics a deposition from the vertical direction onto a horizontal flat mould, namely a deflection of *90°*, for four different punch diameters (*20*, *30*, *40*, *50 mm*). Single strips of prepreg were used as specimens for the test (thickness about *0.195 mm*, length *50-70 mm*, width *5-8 mm*). They were pre-cured in the oven without vacuum to achieve the four different levels of conversion *22*, *31*, *41* and *52%*. The bending test was run at a temperature *20°C* higher than the glass transition temperature. After reaching thermal stability and homogeneity, the unclamped specimen was bent at a down speed of *2 mm/min*. Afterwards, the chamber was cooled below the glass transition temperature, the punch head was raised, and the specimen removed. Because of the slowness of the reaction at the testing temperatures, the degree of cure was reasonably assumed constant throughout the experiment. Four specimens were obtained for each of the *16* cases.

Figure 3. Bending setup

The surface of the specimens was inspected using optical microscopes and pictures were taken. The analysis revealed the presence of in-plane waviness, which was geometrically characterised via the three parameters depicted in Fig. 4. Measured parameters are representative of a set of waves with similar geometry, meaning that each value catches the shape of a group of adjacent waves. Since edges are more subjected to defects related to cutting and handling of the material, any defect close to them was ignored.

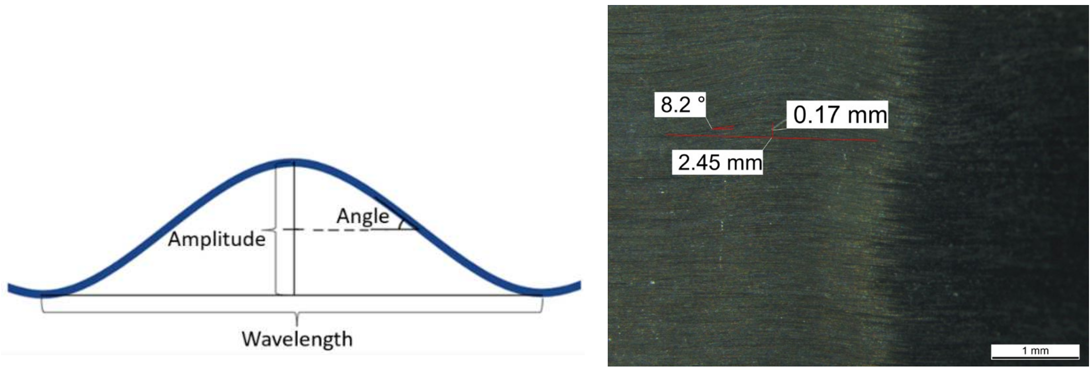

Figure 4. Geometrical parameters of waves

3. Results and discussion

3.1 Resin characterisation

The parameters of the materials models to fit the experimental data for cure kinetics, DiBenedetto and specific heat are reported in Tab. 1. Two practical rules are commonly used to define gelation: the point where dynamic viscosity reaches *10 kPa·s* or where storage and loss moduli cross over [11]. In this study, both methods show similar results and gelation occurs at an averaged degree of cure of *48% ± 7%*.

Table 1: Parameters of the models used for resin characterisation

Parameter	Value	Unit	Parameter	Value	Unit
n	*0.915*	/	C_r	*1.588*	J g^{-1} K^{-1}
m	*0.564*	/	Cr_T	*0.002575*	J g^{-1} K^{-2}
A	*2.1E+10*	s^{-1}	C_g	*1.485*	J g^{-1} K^{-1}
E	*96874*	J mol^{-1}	C	*0.171*	K^{-1}
C	*33.54*	/	σ	*71.82*	K
α_C	*-2.613*	/	σ_T	*-0.7458*	/
α_T	*0.00913*	K^{-1}			
Tg_0	*2*	°C			
Tg_∞	*141*	°C			
λ	*0.48*	/			

3.2 Exothermic overshoot and Finite Element Analysis

The exothermic overshoot was computed from temperature measurements during the cure of the two laminates manufactured in this project. Its maximum was recorded between the middle and the bottom and was equal to *10.0°C* for the standard cure case, while it was equal to *6.4°C* for the multistage cure (reduction of *36%*). These measurements were compared to simulated values in order to validate the HT analysis (in Fig. 5 the comparison in the standard cure case at the centre location of the laminate). The results of the simulations are reported in Fig. 6. The reduction in percentage is quantified using as reference the simulated temperature difference between the middle and the bottom of a standard manufactured laminate without pre-curing at the occurrence of the maximum overshoot, which is represented by the contour maps in Fig. 7. The use of fixed temperature boundary conditions for the nodes in touch with the tool explains why the overshoot in Fig. 7 differs from measured values.

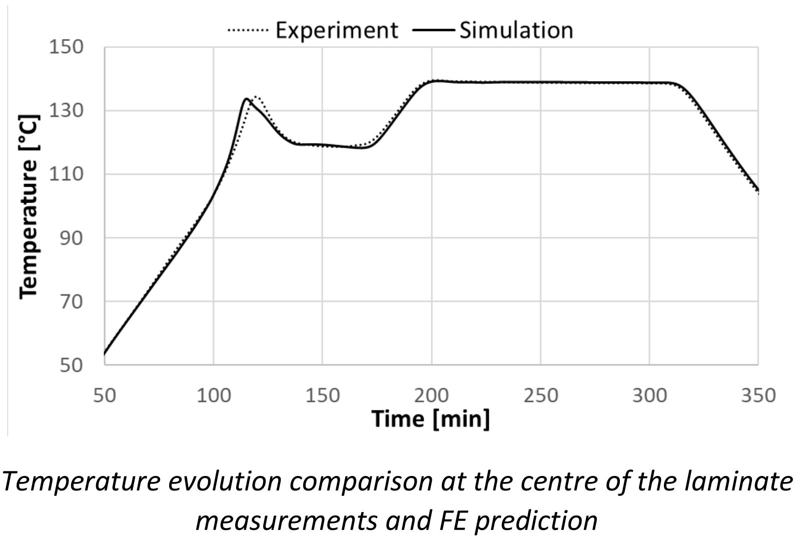

Figure 5. Temperature evolution comparison at the centre of the laminate between measurements and FE prediction

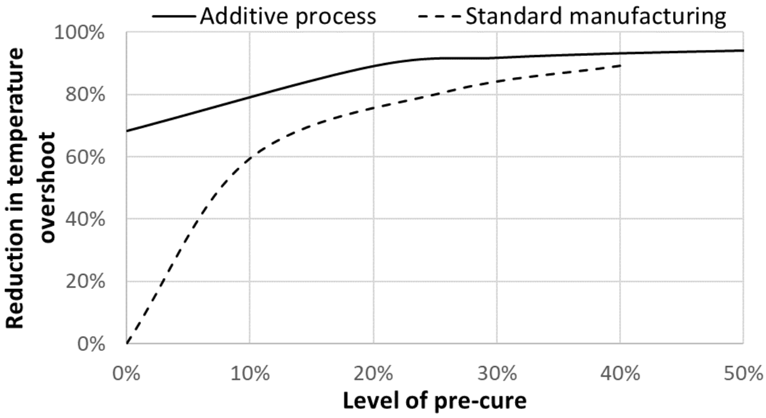

Figure 6. Reduction in temperature overshoot due to pre-cure in AM

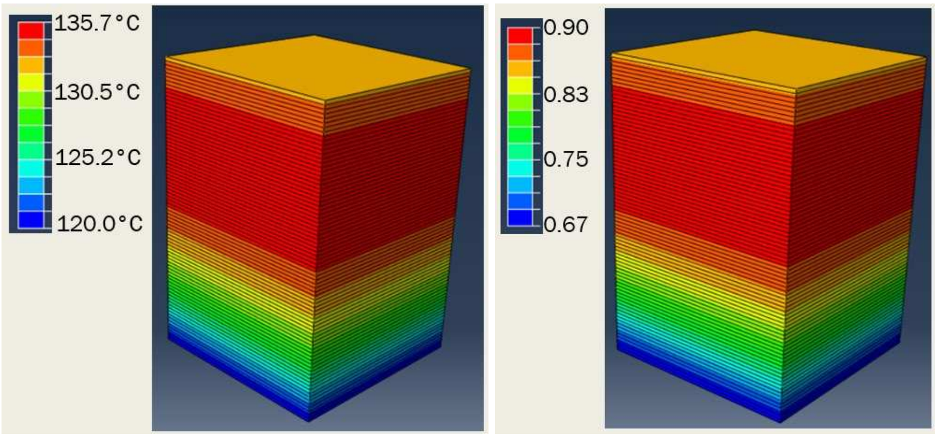

Figure 7. Through thickness results when MRCC is applied: Temperature (left); Degree of cure (right).

From Fig. 6 it can be inferred that the temperature overshoot is strongly reduced by using an additive process. Since the material is being deposited while curing, the process effectively deals with a fraction of the entire thickness resulting in lower temperature overshoot. Moreover, an increasing level of pre-cure translates into a weaker exothermic phenomenon for both processes since chemical potential has been partially exhausted in the pre-cure phase. Finally, beyond *25%* pre-cure level benefits in temperature overshoot reduction become less significant. At the same time, a higher pre-cure level is anticipated to introduce more defects upon deposition, therefore a trade-off is necessary.

3.3 Defects from deposition – in-plane waviness

Optical microscopy revealed the presence of in-plane waviness on the surface of the specimens, the source of which is to be found in the compressive stresses generated during curing and bending that exceed the critical microbuckling stress [7,8]. This analysis assumes the waviness as fully developed along the surface, which makes the approach strongly conservative. The outcomes of the geometrical characterization are plotted against the degree of cure in Fig. 8 using the average value of the four specimens available for each condition. The plot shows no trend between the severity of the waves and the dimension of the punch; this means that there is a margin of freedom to vary that parameter since a smaller compaction roller is more suitable during the printing of concave and complex shapes. On the other side, there is a relationship between the degree of cure and the severity of the waviness. Waves become shorter and wider if the degree of cure increases, or equivalently if the level of pre-cure is higher. Below gelation (*48%* for the system under study) stresses are able to relax. The increasing severity of the waviness shown in Fig. 8 reflects the increasing difficulty of the resin to relieve stresses as gelation is approaching. Another phenomenon leading to this trend is that curing in its first phase is chemical-dominated, therefore compressive stresses induced by resin shrinkage are more pronounced if the cure has lasted longer. Finally, the mismatch in coefficient of thermal expansion (CTE) between fibres and resin during heating and cooling phases generates stresses while testing the specimens. In UD laminates, waviness is expected to have the strongest effect on compressive strength because the component might end up into buckling mode of failure [7,8,13]. It is also proved that the number of wavy plies plays a crucial role and this would occur in every layer since it is generated during the additive deposition of tows. Being aware of the differences between this work and the cited papers [13], it is still possible to state that a waviness with the geometrical characteristics measured for pre-cured specimens up to *30%* should lead to a compressive strength reduction between *2%* and *10%* of the nominal value. Instead, more severe waves like the ones detected for cure levels of *40%* and *50%* might reduce the resistance to compression of a value between *9%* and *24%*.

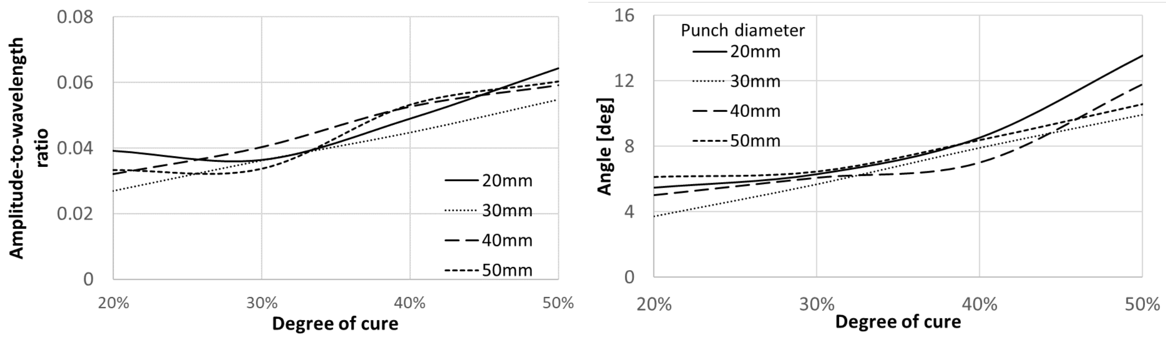

Figure 8. Influence of pre-cure level on in-plane waviness

4. Conclusion and future works

This project reveals that the splitting of the cure in a pre-curing and a post-curing stage in AM has the potential to reduce temperature overshoot generated inside thick CFRP thermosetting composites during their cure. Two competing phenomena are observed. On one hand, pre-curing reduces the temperature overshoot; on the other hand, a higher level of pre-cure induces more severe defects during deposition (i.e. microbuckling). The optimal level of pre-cure is the one that reduces the exothermic overshoot without creating relevant defects during the deposition stage. A level of pre-cure between *20%* and *30%*, for the resin system under investigation, reduces temperature differences inside the material by more than *90%,* generating in-plane waves with a severity that should not compromise the mechanical performances of the component. In order to further progress the understanding of the process under investigation, future research should delve into the characterisation of in-plane waviness generation during the deposition stage and into other types of defects related to this manufacturing technique.

Acknowledgements

This work was supported by the Laboratory for Mechanical Systems Engineering, Swiss Federal Laboratories for Materials Science and Technology (Empa) through the Empa board of directors (project code AP304-2124).

5. References

1. Struzziero G, Nardi D, Sinke J, Teuwen JJ. Cure-induced residual stresses for warpage reduction in thermoset laminates. Journal of Composite Materials 2020; 54(22):3055-3065.
2. Kravchenko OG, Kravchenko SG, Pipes RB. Cure history dependence of residual deformation in a thermosetting laminate. Composites Part A: Applied Science and Manufacturing 2017; 99:186-197.
3. Struzziero G, Teuwen JJ. A fully coupled thermo-mechanical analysis for the minimisation of spring-in and process time in ultra-thick components for wind turbine blades. Composites Part A: Applied Science and Manufacturing 2020; 139:106105.
4. Bogetti TA, Gillespie JW. Process-induced stress and deformation in thick-section thermoset composite laminates. Journal of Composite Materials 1992; 26(5):626-660.
5. Skordos AA, Kratz J. Layer by layer curing (LbL) - Feasibility study. 2018.
6. Struzziero G, Barbezat M, Skordos AA. Assessment of the benefits of 3D printing of advanced thermosetting composites using process simulation and numerical optimisation. Additive Manufacturing 2022; 54:102719.
7. Slaughter WS, Flecks NA. Microbuckling of fiber composites with random initial fiber waviness. Journal of the Mechanics and Physics of Solids 1994; 42(11):1743-1766.
8. Liu D, Fleck NA, Sutcliffe MPF. Compressive strength of fibre composites with random fibre waviness. Journal of the Mechanics and Physics of Solids 2004; 52(7):1481-1505.
9. Datasheet Huntsman - Resin XB 3515 / Aradur® 1571 / Accelerator 1573. 2009.
10. Karkanas PI, Partridge IK. Cure modeling and monitoring of epoxy/amine resin systems. i. cure kinetics modelling. Journal of applied polymer science 2000; 77(7):1419-1431.
11. Zarrelli M, Skordos AA, Partridge IK. Investigation of cure induced shrinkage in unreinforced epoxy resin. Plastics, Rubber and Composites: Macromolecular Engineering 2002; 31(9):377-384.
12. Yan X. Finite element modeling of curing of epoxy matrix composites. Journal of applied polymer science 2007; 103(4):2310-2319.
13. Mandell J, Samborsky D, Wang L. Effects of fiber waviness on composites for wind turbine blades. International SAMPE symposium and exhibition 2003; 2653-2666.